SUPERCONDUCTIVITY, INCLUDING HIGH TEMPERATURE SUPERCONDUCTIVITY

Stochastic resonance in superconducting loops containing Josephson junctions. Numerical simulation

A. M. Glukhov, O. G. Turutanov,[a] V. I. Shnyrkov, and A. N. Omelyanchouk

B. Verkin Institute for Low Temperature Physics and Engineering, National Academy of Sciences of Ukraine, pr. Lenina 47, Kharkov 61103, Ukraine
(Submitted February 21, 2006)
Fiz. Nizk. Temp. **32**, 1477–1487 (Decemeber 2006)

A numerical simulation of the stochastic resonance is carried out in the adiabatic approximation in overdamped systems based on superconducting loops closed by a weak link. The systems under consideration include a single-ring rf SQUID, two rings coupled by a common magnetic flux, and a ring closed by a 4-terminal Josephson junction. It is shown that coupling of single SQUID rings enhances the gain and the signal-to-noise ratio. These effects can be used to create new stochastic SQUID antennas for measurements of harmonic and quasi-harmonic signals. The stochastic resonance in 4-terminal SQUIDS exists even at values of the dimensionless inductance $l<1$. *© 2006 American Institute of Physics*. [DOI: 10.1063/1.2400686]

INTRODUCTION

The concept of "stochastic resonance" (SR) was first introduced in Refs. 1–3. The SR phenomenon is manifested in an increase of the response of a determinate dynamical system to a weak periodic signal and an increase of the signal-to-noise ratio when an additional noise of a certain optimum intensity is introduced in the system. The effect arises because of pumping of energy from the stochastic process (noise) into energy of the determinate process (signal) and leads to a seeming violation of the thermodynamic prohibition of a decrease of entropy. The paradox vanishes when it is taken into consideration that the system has input and output parameters, which automatically make it an open system.[4,5] The SR effect was first explained for bistable systems under the assumption of their adiabaticity (the frequency of the periodic signal is significantly lower than the inverse relaxation time of the system) in terms of two-state models.[6] Later it was observed and studied theoretically with the use of the more general approach of linear response theory[7,8] in systems with a single stable state at high signal frequencies.[9] SR is also observed in threshold systems.[10] Thus the system need not necessarily be a dynamical one;[11] it is sufficient to have only nonlinearity of its "transfer function." The SR effect has also been observed in a Josephson percolation medium.[12]

As is shown in Refs. 13 and 14, the conditions necessary for the onset of SR are easily fulfilled in superconducting quantum interference devices (SQUIDs), which are usually used to register broadband low-frequency signals. In the broadband detection regime the values of the sensitivity of dc and rf SQUIDs are very high and practically approach the quantum limit. Progress in technology of preparing high-quality Josephson junctions of small area, improvement of the parameters of transistors, and refinement of the electrical circuits for registration have permitted the achievement of record-high values of the sensitivity in the creation of various devices, including multichannel receiving devices for measuring biomagnetic fields, susceptibility, low-frequency radar, geophysical apparatus, etc.

It is perfectly obvious that some practical applications (magnetoencephalography, geophysical research) do not require broadband reception, since the information signal to be registered lies in a narrow frequency range. For example, in nondestructive monitoring systems,[15] low-frequency radar units,[16] and systems for measuring the magnetic susceptibility of biological objects[17] the signal to be measured is concentrated at a single frequency, and a broadband input antenna is an impediment to realizing the highest possible sensitivity of the SQUID. In such measurements the SR effect can be extremely useful for narrowing the input band of the antenna, and for improving the signal-to-noise ratio through the stochastic amplification of weak signals. It can be expected[18] that when the area of the receiving antenna is filled with intercoupled stochastic oscillators[19] (e.g., based on a superconducting quantum interferometer with one Josephson junction) the SR will lead to enhancement of the response to a weak signal. However, the behavior of such a dynamical system on the whole will depend on many parameters, and to search for the optimum strategy experimentally is extremely laborious. Therefore, it is of significant interest to carry out a theoretical search for the optimal characteristics of both autonomous SR oscillators and coupled dynamical systems.

This paper is devoted to a numerical simulation of SR in a system of coupled rf SQUID rings and in a superconducting ring closed by a 4-terminal weak link.[20]

In the interests of practical applications, we have studied the response of rf SQUID rings to a weak harmonic signal of very low frequency ($\sim$1 Hz). At the same time, it is known that for a typical SQUID ring the characteristic relaxation time of the flux, $\tau_L = L/R_J \sim (10^{-9}-10^{-11})$ s (L is the inductance of the ring, and R_J is the normal resistance of the weak link). Such a large difference of the characteristic times of the signal and system permits one to use the adiabatic ap-

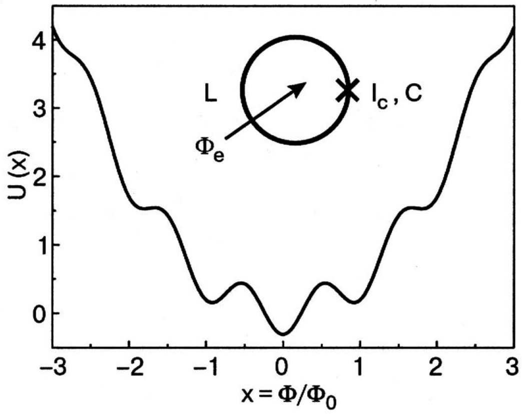

FIG. 1. Potential function of a superconducting loop containing a Josephson junction. The hysteresis parameter β=12, the external magnetic flux x_{dc}=0. Inset: scheme of the rf SQUID ring; L is the inductance of the ring, Φ is the magnetic flux through the ring, and I_c and C are the critical current and the capacitance of the Josephson junction, respectively.

proximation and avoid direct solution of the equations of motion. The approach developed in the present study proposes to construct a potential surface that depends on both a periodic signal and a random signal and to trace the evolution of its topology and shape under the influence of these external signals. The shape of the potential surface at each point in time (with the pre-history taken into account) uniquely determines the state of the system. Thus one constructs a time series of states of the system and subjects it to further analysis.

MODEL OF STOCHASTIC RESONANCE IN A SINGLE rf SQUID RING

The SR effect has been studied most fully in systems having two stable states separated by a potential barrier. To check the workability of the proposed calculation technique, let us go through a numerical simulation of such a system while elucidating the SR mechanism along the way. Let us consider a superconducting loop containing a Josephson weak link, which we shall refer to as an rf SQUID ring (inset in Fig. 1).

Taking into account that at finite temperatures both a supercurrent and quasiparticle current pass through the Josephson junction, i.e., using the well-known resistively shunted Josephson junction (RSJ) model, one can write an equation for the magnetic flux Φ inside the ring:[21]

$$\left(LC\frac{d^2}{dt^2}+\tau_L\frac{d}{dt}+1\right)\frac{\Phi(t)}{\Phi_0}+\frac{\beta}{2\pi}\sin\frac{2\pi\Phi}{\Phi_0}=\frac{\Phi_e(t)}{\Phi_0}, \qquad (1)$$

where C is the capacitance of the ring (concentrated at the Josephson junction), $\tau_L=L/R_J$ is the magnetic relaxation time of the ring, I_c is the critical current of the Josephson junction, $\beta=2\pi LI_c/\Phi_0$ is the hysteresis parameter (hysteresis is observed on the $\Phi(\Phi_e)$ curve for $\beta>1$), and Φ_0 is the magnetic flux quantum.

If a microbridge or point contact is used as the Josephson junction, its capacitance will be vanishingly small ($C\sim 10^{-15}$ F), and its resistance in the normal state will have a value $R_N\sim 1\ \Omega$. If a tunnel junction is used, it will be shunted by a small resistance in order to reduce the influence of the junction capacitance and thereby shorten the duration of the transient process in the ring. Thus, since the inductance L of the ring usually lies in the range 10^{-9}–10^{-11} H, it turns out that the term with the second derivative in Eq. (10) is much smaller than the other terms and can be neglected.

We separate the external flux $\Phi_e(t)$ into a dc component Φ_{dc}, a periodically alternating signal Φ_{ac} with amplitude a and frequency f_s, and a stochastic part Φ_N:

$$\Phi_e(t)=\Phi_{dc}+\Phi_{ac}+\Phi_N(t);\quad \Phi_{ac}=a\Phi_0\sin(2\pi f_s t), \qquad (2)$$

where for $\Phi_N(t)$ we use a Gaussian random process with zero mean and variance D:

$$\Phi_N(t)=\Phi_0\xi(t),\ \langle\xi(t)\xi(t')\rangle=2D\delta(t-t').$$

The details of the numerical realization of the periodic signal and noise component will be discussed below.

Normalizing the magnetic flux by the flux quantum Φ_0 and introducing the notation

$$x_\alpha=\Phi_\alpha/\Phi_0, \qquad (3)$$

where α is any of the subscripts, we write the equation of motion of the system:

$$\tau_L\frac{dx}{dt}+\frac{\partial U(x,t)}{\partial x}=0. \qquad (4)$$

The time dependence of the potential of the system is determined by the time evolution of the external flux (2) normalized according to Eq. (3):

$$U(x,t)=\frac{1}{2}(x-x_e(t))^2-\frac{\beta}{4\pi^2}\cos 2\pi x, \qquad (5)$$

where the normalized external flux

$$x_e(t)=x_{dc}+a\cos(2\pi f_s t)+\xi(t). \qquad (6)$$

We note that here all of the time dependence can be transferred to the potential because of the adiabatic condition $f_s\ll 1/\tau_L$. As we have said, in real SQUID applications for signal frequencies in the interval 1–1000 Hz this condition holds to good accuracy. Here, of course, we also impose restrictions on the noise band, the upper frequency boundary of which must also be much less than τ_L.

The shape of the potential $U(x)$ of a SQUID ring in the case $\beta>1$ and in the absence of an additional external flux (x_e=0) is shown in Fig. 1. The local minima of the potential correspond to stable states of the ring, separated by energy barriers.

The position and number of extrema of the potential are determined from the condition

$$\frac{dU(x)}{dx}=0, \qquad (7)$$

$$x-x_{dc}+\frac{\beta}{2\pi}\sin 2\pi x=0. \qquad (8)$$

To obtain a double-well potential symmetric with respect to a change of the external magnetic flux, one should set $x_{dc}=1/2$, so and then the positions of the extrema will be solutions of the transcendental equation

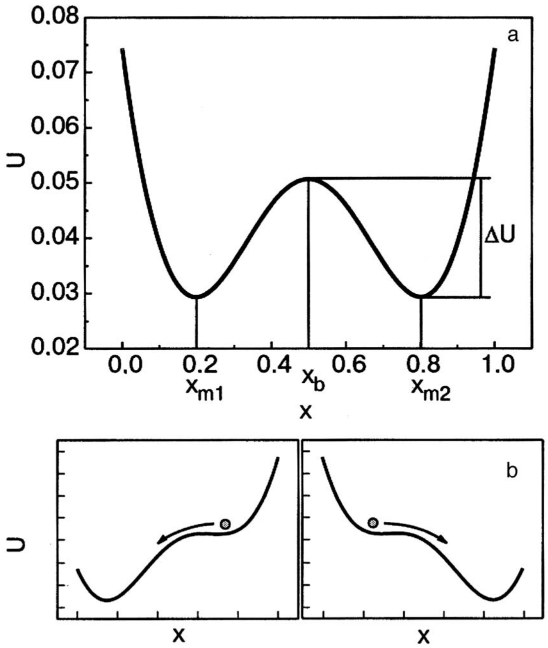

FIG. 2. Symmetric bistable potential of the rf SQUID ring for $\beta=2$ and $x_{dc}=0.5$; the values of the flux corresponding to the minima of the potential (x_{m1},x_{m2}), the middle of the barrier (x_b), and the potential barrier height ΔU (a). A diagram of the transition of the system from one stable state to another upon the warping of the potential by an external magnetic flux (b).

$$x_m = \frac{1}{2} - \frac{\beta}{2\pi}\sin 2\pi x_m. \tag{9}$$

It follows from Eq. (9) that the potential contains not more than two minima at values of β in the interval from 1 to ~ 7.7 (Fig. 2a), while the system has two stable states separated by a potential barrier, making possible the existence of SR in it. We shall specify such a potential in our simulation of the behavior of a single-ring rf SQUID. We note that SR should also exist in a multistable system with a multiwell symmetric potential, but the analysis of such a situation is considerably more complicated. In all the papers known to us the authors have restricted consideration to only two adjacent minima of the potential. Following those papers, we shall assume that for arbitrary β the change of the magnetic flux in the ring is sufficiently small that it does not cause transitions of the system into more remote wells. We also note that it is possible to symmetrize the potential of the ring at zero external magnetic flux by using a π junction[22] instead of the usual Josephson junction; in such a junction in the ground state with zero current the phase difference of the order parameter is equal to π, and a flux equal to $\Phi_0/2$ exists in the ring. For practical applications this method is technologically easier than the specification of an external magnetic flux.

Using this potential as an example, one can explain the essence of the SR effect as follows. Initially, in the absence of noise, the system (particle) is found in one of two local potential energy minima (see Fig. 2a), executing small intrawell oscillations under the influence of a weak periodic force applied to it (a signal). This signal causes a periodic tilt of the potential well to one side and then the other, lowering the barrier somewhat. The amplitude of the signal is insufficient for a transition of the system across the barrier into the second local minimum of the potential. When noise is added to this system there is a finite probability that the system will be transferred across the barrier into the other well (when the instantaneous warping of the potential is sufficient to make one of the local minima vanish); see Fig. 2b. This probability depends on the barrier height and increases with increasing noise intensity (for white noise with a Gaussian distribution the term "intensity" is understood to mean the variance of the distribution). The mean frequency of escape of a particle from a well (and, hence, the frequency of hops to the other well) under the influence of noise in a highly damped system was determined by Kramers,[23] and for white noise, parabolic potential wells, and relatively high barriers it is given by the Arrhenius law:

$$r_k = \frac{\omega_0\omega_b}{2\pi\gamma}\exp\left(-\frac{\Delta U}{D}\right), \tag{10}$$

where $\omega_0=\sqrt{\frac{U''(x_m)}{m}}$ is the frequency of oscillations about the bottom of a well, $\omega_b=\sqrt{\frac{U''(x_b)}{m}}$ is the frequency of oscillations at the local maximum (at the barrier); m is the mass of the oscillating particle, γ is the coefficient of viscous friction (dissipation), ΔU is the barrier height, and D is the noise intensity. If the noise is of a thermal origin, then $D=k_BT$.

Since the application of a periodic signal causes the potential barrier to become a periodic function of time, the transition probability, which determines the output signal, also begins to depend periodically on time. When, with increasing noise intensity, the Kramers frequency becomes twice the frequency of the periodic signal, a "synchronization" of the stochastic and periodic processes occurs: *on average* the hops caused by the noise occur "in phase" with the periodic signal, and in the spectrum of the system one observes an increase of the power of the output signal at the frequency of the weak input signal. Thus the noise facilitates interwell transitions at the times of the peak values of the useful signal. We note that, because of the strong damping the system does not have any characteristic oscillations; all of the processes in it are of a relaxation character.

The above-described behavior of a superconducting ring including a Josephson junction was investigated using a numerical model with the potential (5) and external signal (6). For convenience the constant bias $x_{dc}=1/2$ applied to symmetrize the potential was eliminated from Eq. (5) by the change of variables $(x-1/2)\to x$.

NUMERICAL SIMULATION TECHNIQUE AND THE RESULTS FOR A SINGLE RING

The numerical simulation procedure producing the results shown in Fig. 3 consisted of the following. A given time interval was divided into a large number of subintervals equal to some power of 2 (usually $2^{15}=32768$) for convenience in the subsequent Fourier analysis. At each given point in time the values of the sinusoidal periodic signal and the noise were specified. In most of the calculations the signal frequency f_s was equal to 2–4 Hz and the signal amplitude $a=0.01-0.3$ (in units of Φ_0). To obtain noise with a Gaussian distribution, zero mean, and variance D (which determines the noise intensity), a random number generator

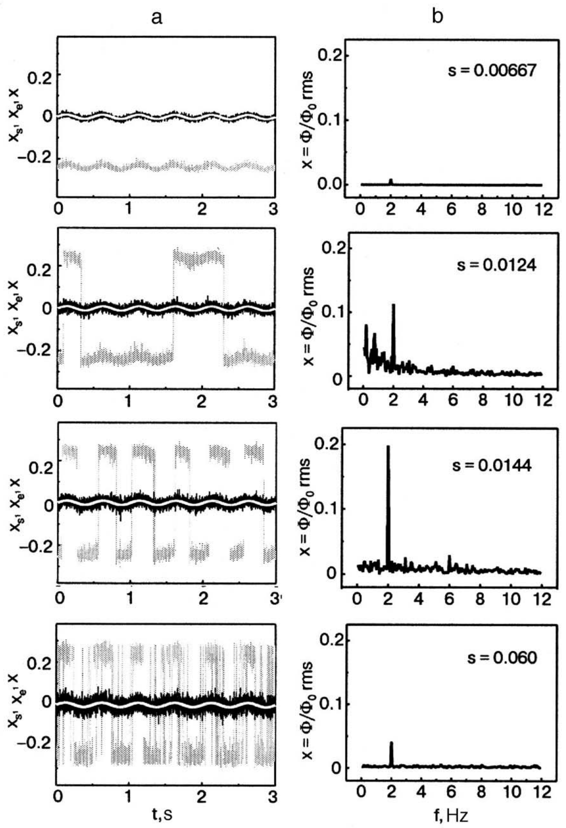

FIG. 3. Time series of a periodic input signal x_s (white curves), the signal with noise, $x_e = x_s + x_N$ (black), and the output signal x (gray) (a); the Fourier spectra of the output signal at different noise levels s (b).

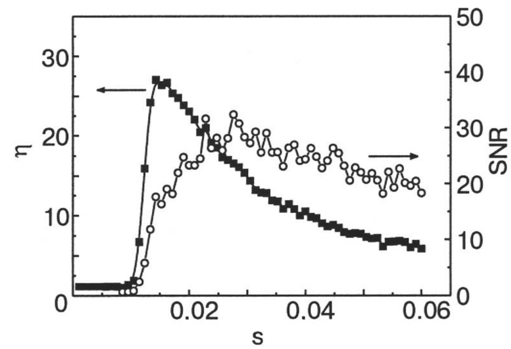

FIG. 4. Dependence of the flux gain and signal-to-noise ratio on the noise level in a one-ring rf SQUID. Parameter $\beta = 1.5$, input signal amplitude $a = 0.01$, signal frequency $f_s = 2$ Hz, noise cutoff frequency $f_c = 2048$ Hz, and number of points in the time series 32768. The curve of the SNR does not appear smooth because of the scatter in the determination of the position of the noise shelf.

with a repetition period of around 2^{90} was used. The noise spectrum is limited from above by a digital filter. The cutoff frequency of the noise was chosen much higher than the signal frequency and, hence, the mean frequency of interwell transitions when the SR effect is realized. Then the number and position of the minima of the potential function are determined at every point in time t_n. If there are two minima (Fig. 2a) then it is assumed that the state of the system has not changed, and it remains in the same well, only with a slight coordinate shift (this situation corresponds to intrawell oscillations). If the potential well is warped so that the combined effect of the periodic and noise signals leaves only a single minimum, the system is transferred into it (if hitherto it was at the other minimum; Fig. 2b), and the value of the normalized flux corresponding to this minimum is assigned to it. As a result, at different noise levels one obtains time series close to a telegraph signal (Fig. 3a). One can eliminate the influence of the intrawell oscillations and obtain a real telegraph signal by filtering the time series by the two-states method,[6] but further calculation shows that this is unnecessary, since the final curves of the flux gain and signal-to-noise ratio remain practically the same as without filtering.

This time series is subjected to a fast Fourier transform (FFT), yielding the spectra of the mean-square deviation of the output signal (the flux in the ring; Fig. 3b). With growth of the noise (from top to bottom in Fig. 3) the behavior of the system changes qualitatively. At a low noise level, hops from one potential well to the other are practically absent, and small intrawell oscillations corresponding to the input signal are observed (the first pattern in Fig. 3a). With increasing noise, hops between wells begin, and a noticeable peak of the signal at the fundamental frequency appears (the second pattern in Figs. 3a and 3b, respectively). At a certain optimal noise level a statistical "synchronization" of the noise and signal appears, the hops become quasi-periodic, and the height of the peak in the output Fourier spectrum at the fundamental frequency grows strongly against the background of the subsiding noise shelf (the third pattern in Fig. 3a and 3b). A high noise level destroys the correlation of the hops with the periodic signal, and the height of the peak at the fundamental frequency in the Fourier spectrum falls off (the fourth picture in Fig. 3b).

Figure 4 shows a plot of the flux gain η, defined as the ratio of the output to the input signal at the fundamental frequency, as a function of the standard deviation of the noise $s \equiv D^{1/2}$ (the noise level). Also shown is the behavior of the signal-to-noise ratio (SNR) as a function of s. The value of the SNR was calculated as the ratio of the height of the main peak in the Fourier spectrum to the mean height of the noise shelf beneath it. The curves have the "classic" form for the SR effect.[4,5,13,14] We note that, generally speaking, the values of the noise level at which the maxima are observed on the curves of the gain and signal-to-noise ratio do not coincide. A noise level $s < 0.01$ is insufficient for transition through the barrier with appreciable probability (only intrawell oscillations occur), and therefore the determination of the signal-to-noise ratio at such small values of the noise is incorrect.

A characteristic feature of the SR is the high sensitivity of the spectrum of the output signal to a bias of the input flux. Since the process of stochastic amplification is of a nonlinear character, the spectrum of the output signal contains higher harmonics in addition to the fundamental frequency (Fig. 5). In the absence of a constant bias flux ($x_{dc} = 0$) the potential $U(x)$ is symmetric, and even harmonics are absent from the spectrum (Fig. 5a). By applying a constant bias one can achieve a situation in which odd harmonics (not counting the fundamental frequency) are absent from the spectrum; Fig. 5c. Figure 6 shows the dependence of the amplitudes of the first three harmonics of the signal as func-

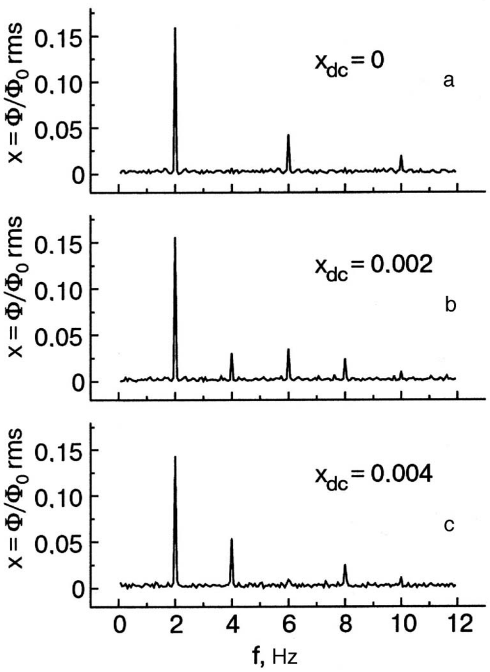

FIG. 5. Even and odd harmonics in the Fourier spectrum of the output signal at different levels of the constant bias flux. The noise intensity is equal to that value at which the maximum stochastic amplification of the signal is observed.

tions of the dc bias flux; they are in good agreement with the results given in Ref. 13.

SIMULATION OF THE STOCHASTIC RESONANCE IN COUPLED RINGS

Consider the situation in which rings lie side by side in the same plane and have a magnetic coupling between them that is determined by their mutual inductance. Here part of the flux of one ring falls into the other ring, and vice versa.

In this case the potential is written as the sum of the individual potentials of the rings and an overlap term taking the interaction into account:

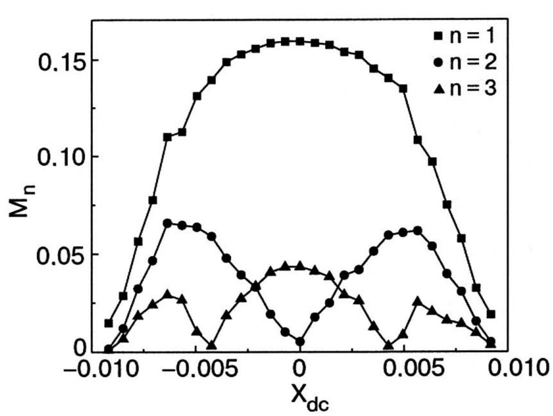

FIG. 6. Values of the first three harmonics of the main signal in the output Fourier spectrum as a function of the input bias flux x_{dc}; β=1.5. The noise intensity is equal to that value at which the maximum stochastic amplification of the signal is observed.

$$U(x_1,x_2)=\frac{(x_1^2+x_2^2)}{2}+\frac{(\beta_1\cos 2\pi x_1+\beta_2\cos 2\pi x_2)}{4\pi^2} - kx_1x_2, \tag{11}$$

where x_1, x_2 and β_1, β_2 are normalized fluxes and the hysteresis parameters in the first and second rings, respectively, while k is the coupling strength via the flux between rings (the normalized mutual inductance). We recall that x_1 and x_2 have been shifted by 0.5 for symmetrization of the potential. The negative sign of the cross term means that the fluxes of the rings are directed counter to each other.

Figure 7 shows the shape of the potential surface for a system of two coupled rings at different values of the hysteresis parameters β_1, β_2 (Fig. 7a and 7b) and coupling coefficient k (Fig. 7c and 7d).

The superposition of a sinusoidal periodic signal and noise, as in the case with one ring, leads to a time-dependent warping of the potential:

$$U(x_1,x_2,t)=\frac{[x_1-x_{e1}(t)]^2+[x_2-x_{e2}(t)]^2}{2} + \frac{(\beta_1\cos 2\pi x_1+\beta_2\cos 2\pi x_2)}{4\pi^2} - kx_1x_2, \tag{12}$$

where the external fluxes $x_{e1}(t), x_{e2}(t)$ are determined by formula (6) in which the constant bias x_{dc} is set equal to zero.

All of our further results are shown for the case $x_{e1}(t)=x_{e2}(t)=x_e(t)$ as having the most practical significance.

Figure 7e and 7f shows two "phases" of the tilt of the potential by an external flux.

As we see in Fig. 7, in the case of a pair of coupled rings the system can land in one of four wells of the potential surface.

The procedure for determining the present state of the system in this case is somewhat more complex. One takes into account the vanishing of the barrier between the well in which the system is located at the given time and the neighboring wells. If both barriers vanish simultaneously, then the probability of transition of the system into the neighboring wells is the same for both, and the new present state is chosen from them at random. In the course of the simulation it became clear that in the presence of four wells the transition of the system occurs not directly along the diagonals but with an intermediate hop through one of the nearest minima, since the height of the barrier between nearest minima is lower than between wells along a diagonal.

The time dependence obtained for the total flux in the rings, as in the case of a single ring, was subjected to FFT. In the same way, the flux gain and the signal-to-noise ratio were calculated from the height of the spectral peak at the frequency of the useful signal. The resulting dependence of η on the noise level s and coupling constant k for the case of identical rings is shown in Fig. 8a, and for the case of rings with different hysteresis parameters β, in Fig. 8b. As a calculation shows, the signal-to-noise ratio behaves in an analogous manner, but the scatter of the calculated points is relatively large because of the large scatter in the determination of the noise shelf.

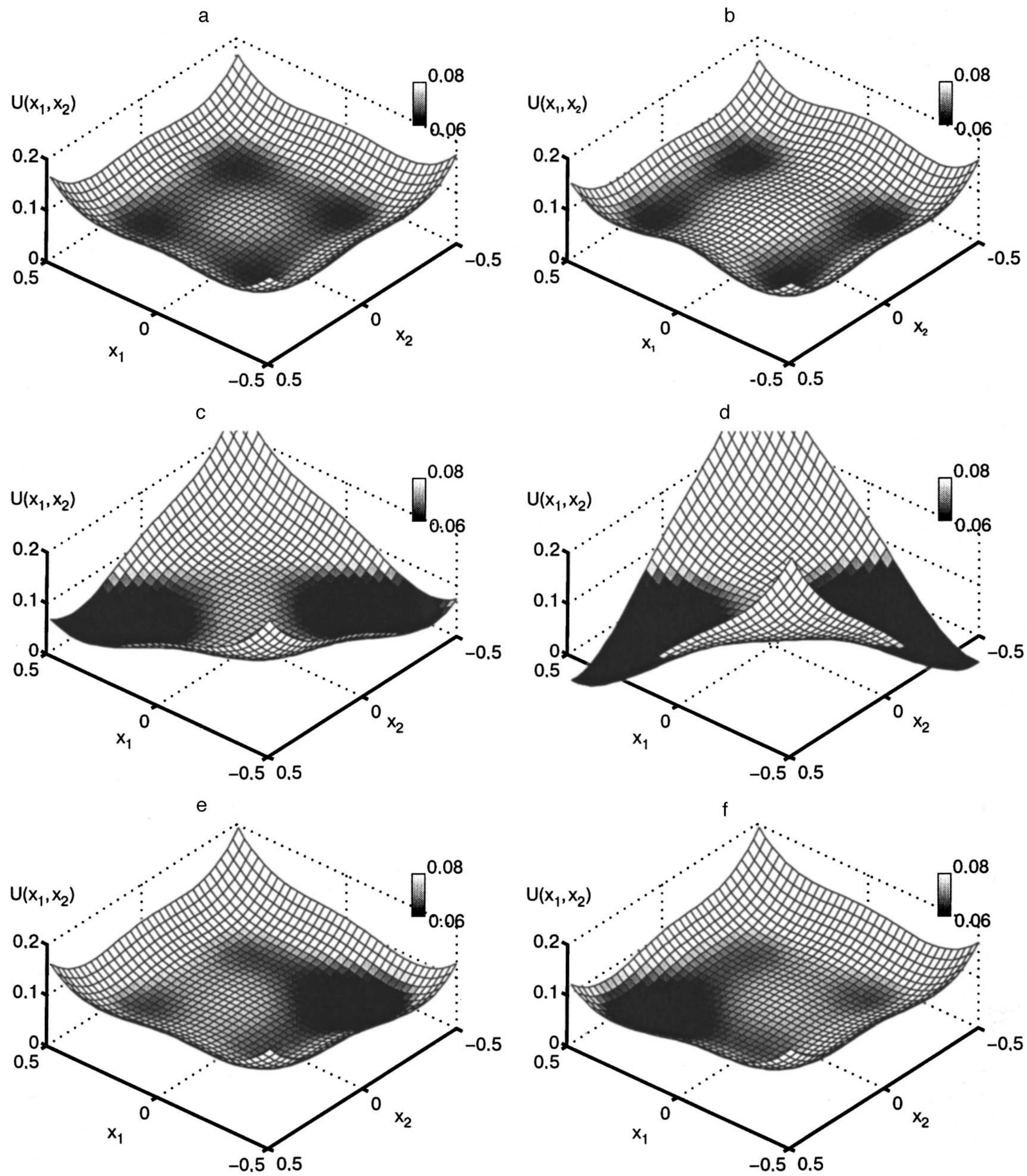

FIG. 7. Potential surface $U(x_1,x_2)$ for two coupled rf SQUID rings in the absence of additional bias, input signal, and noise at the following parameter values: $\beta_1=\beta_2=1.5$, $k=0$ (a); $\beta_1=1.5$, $\beta_2=2$, $k=0$ (b), $\beta_1=\beta_2=1.5$, $k=0.4$ (c); $\beta_1=\beta_2=1.5$, $k=0.9$ (d), and with biasing by an external signal for $\beta_1=\beta_2=1.5$, $k=0.1$, $x_e=-0.02$ (e); $\beta_1=\beta_2=1.5$, $k=0.1$, $x_e=+0.02$ (f).

If the hysteresis parameters β_1 and β_2 of the rings are different, then the curve of the gain as a function of the noise level $\eta(s)$ exhibits a feature corresponding to resonance of the ring with the lower β in addition to the maximum corresponding to the total resonance of the two rings. It is seen that a higher gain is reached in the case of identical rings. In both cases the flux gain increases with increasing coupling strength k between rings. The gain in the case of strong coupling is significantly greater than in the case of a single ring (cf. Figs. 4 and 8a). This effect can be given a transparent interpretation in terms of the geometry of the potential surface. With increasing coupling coefficient two of the four minima gradually vanish (the transition from a surface of the form in Fig. 7a to the surfaces in Fig. 7b and 7c), and now the behavior of the coupled pair is similar to the behavior of the single ring, with the only difference being that the minima lie along the diagonal, and the distance between them is greater than in a single SQUID, which makes for an increase in the SR effect. Based on this geometric interpretation, one expects that with increasing number of coupled rings the gain should increase $\sim N^{1/2}$, where N is the number of coupled rings.

MODELING THE STOCHASTIC RESONANCE IN A 4-TERMINAL SQUID

The SR in a 4-terminal SQUID[24] at relatively high signal frequencies was considered in Ref. 25. That has made it possible to obtain the time evolution of the total magnetic flux in a ring by direct numerical solution of the equation of motion in the presence of noise. At low signal frequencies the direct solution of the equation of motion becomes an extremely

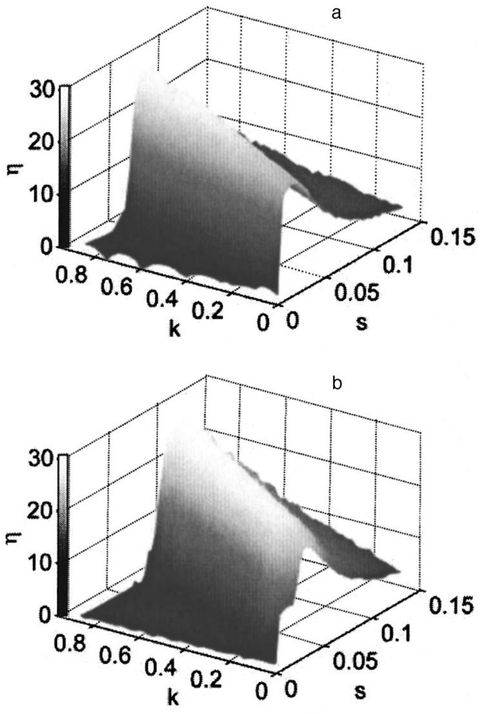

FIG. 8. Flux gain η as a function of the noise level s and coupling coefficient k for identical rings (a) and different rings (b). Signal amplitude $a=0.03$, signal frequency $f_s=2$ Hz, hysteresis parameters $\beta_1=\beta_2=1.5$ (a); $\beta_1=1.5$, $\beta_2=2$ (b).

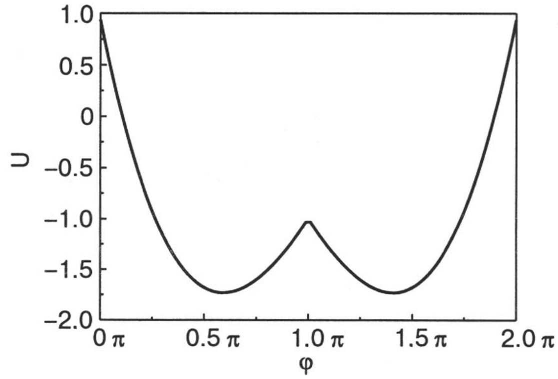

FIG. 9. Potential of a 4-terminal SQUID for $l=1$, $I=0$, $\varphi_e=\pi$.

protracted process, since, because of the presence of a noise component, one cannot take advantage of methods of solution of differential equations developed for stiff systems. However, numerical simulation in the adiabatic approximation does not entail any particular complication. If we restrict consideration to the case of zero transport current I and take into account that $\theta=0$, the potential describing a 4-SQUID,[24]

$$U\left(\theta,\varphi,\chi \middle|_{I,\varphi^e}\right)=\frac{(\varphi-\varphi^e)^2}{2l}-I\theta-\cos^2\frac{\theta}{2}-\cos^2\frac{\varphi}{2}$$

$$-2\cos\frac{\theta}{2}\cos\frac{\varphi}{2}\cos\xi, \tag{13}$$

can be written in the form

$$U(\varphi)=\frac{(\varphi-\varphi^e)^2}{2l}-1-\cos^2\frac{\varphi}{2}-2\left|\cos\frac{\varphi}{2}\right|. \tag{14}$$

This potential (Fig. 9) is not equivalent to the potential of an rf SQUID ring containing an ordinary 2-terminal Josephson junction. Unlike the usual SQUID, here the potential remains double-well even when the dimensionless inductance parameter $l<1$.

Indeed, a numerical simulation shows that SR is present in such a ring. Figure 10 shows the flux gain for a sinusoidal signal as a function of the noise level.

Detailed study of SR in a 4-terminal SQUID, including the case when there is a transport current through the weak link, is beyond the scope of this paper.

STOCHASTIC ANTENNAS

At this time even the standard SQUID-based receivers have an intrinsic sensitivity at the level 10^{-32}–10^{-31} J/Hz. However, the realization of such a sensitivity is in many cases limited by noise in the antenna circuits, which in the majority of devices are broadband. To reduce the influence of external electromagnetic fields the input circuits of SQUIDs are designed as gradientometers and are partially filtered by means of *RL* filters. However, the *RL* filters increase the spectral density of noise in the antenna, and the gradientometers degrade the sensitivity of the receivers in relation to sources located in the far zone.[16] These difficulties can be partially overcome with the use of the SR effect in the antenna units.

It follows from the results presented above that if the area of the receiving antenna is filled with one or several SR loops (Fig. 11), then the current induced in the antenna will have frequency dependence with a maximum at the resonance frequency. Since that maximum depends on the noise power, the frequency characteristic of the antenna can be tuned within certain limits to the frequency of an external harmonic signal to obtain a maximum transformation ratio of the magnetic flux in the SQUID at a specified frequency. Interestingly, in the region of infrared frequencies lying below the frequency of the stochastic resonance, such antennas have a low transformation ratio and act as filters of a sort, while at the chosen SR frequency one can even achieve weak-signal gain. In some kinds of SQUID-based receivers (see, e.g., Refs. 15–17) low-frequency magnetic fields are

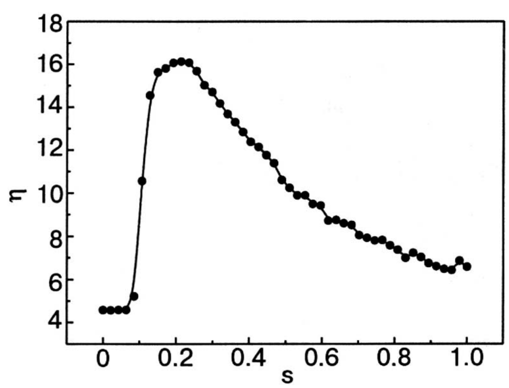

FIG. 10. Flux gain η as a function of the noise level s in the ring of a 4-terminal SQUID. Parameters: $l=0.5$, $f_s=2$ Hz, $a=0.25$.

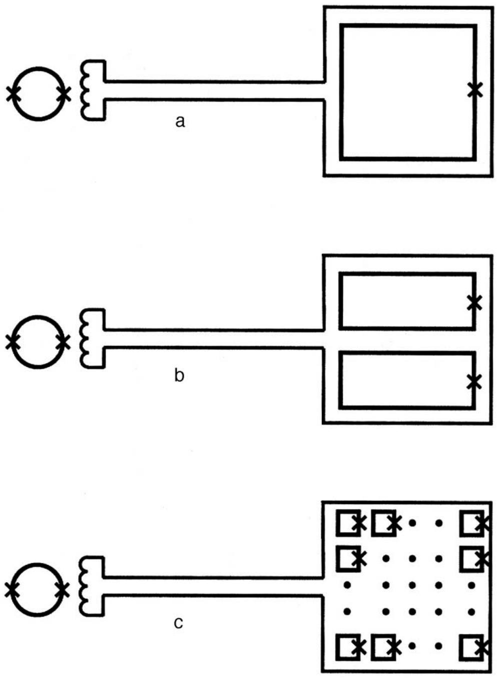

FIG. 11. Possible configurations of stochastic antennas for receiving weak quasi-harmonic signals with the use of SQUIDs: a,b—antennas for SQUID microscopes, c—antennas for low-frequency radar, geophysical magnetometry, and biomagnetic measurements.

used to probe the objects under measurement, and in this case useful information is contained in the reflected harmonic (or quasi-harmonic) signal, which can be amplified with the use of SR antennas.

The above analysis shows that when the area of planar antennas are filled with a large number of stochastic loops, it is important to use systems with a small scatter of parameters. For example, one of the requirements is a minimum scatter with respect to the critical current, the amplitude of which controls the height of the potential barrier. This condition is very well satisfied in π junctions, which were studied in detail in Ref. 22. Moreover, the ground state of a superconducting ring closed by such a π junction is a state with a symmetric double-well potential, as is needed for SR. Since the characteristic normal resistance of such junctions is rather large $(R \sim 1\ \Omega)$, the characteristic time L/R does not restrict the stochastic dynamics under consideration.

CONCLUSION

The phenomenon of stochastic resonance in systems containing a superconducting loop with a Josephson weak link enables one to obtain additional amplification of a weak magnetic signal. The coupling of even two such loops together by a common magnetic flux leads to an appreciable increase (by nearly a factor of 1.5) in the flux gain and signal-to-noise ratio. It is expected that as the number of coupled rings increases, the gain and signal-to-noise ratio will grow by approximately a square-root law. This effect can be used to create fundamentally new stochastic SQUID antennas that permit one to obtain a relatively large gain in the presence of noise. The use of a π junction as a weak link makes it possible to avoid the need for additional bias by an external constant flux.

Stochastic resonance in a superconducting ring containing a 4-terminal Josephson junction (a 4-terminal SQUID) is interesting from the standpoint that the parameters of a 4-SQUID can be controlled by changing the conditions for the appearance of SR. This, in principle, permits one to create a stochastic amplifier with a tunable signal band and with tuning of the working point under a given noise level (external and internal).

A convenient method for studying SR in these and other systems in the adiabatic limit is numerical simulation based on analysis of the changes of the geometry of the potential surface of the system as a result of external influences.

[a]Electronic mail: turutano@ilt.kharkov.ua

[1]R. Benzi, A. Sutera, and A. Vulpiani, J. Phys. A **14**, L453 (1981).
[2]J.-P. Eckmann, L. Thomas, and P. Wittwer, J. Phys. A **14**, 3153 (1981).
[3]C. Nicolis and G. Nicolis, Tellus **33**, 225 (1981).
[4]L. Gammaitoni, P. Hänggi, P. Jung, and F. Marchesoni, Rev. Mod. Phys. **70**, 223 (1998).
[5]V. S. Anishchenko, A. B. Neiman, F. Moss, and L. Schimansky-Geier, Usp. Fiz. Nauk **169**, 7 (1999) [Phys. Usp. **42**, 7 (1999)].
[6]B. McNamara and K. Wiesenfeld, Phys. Rev. A **39**, 4854 (1989).
[7]M. Dykman, P. McClintock, R. Manella, and N. Stocks, JETP Lett. **52**, 141 (1990).
[8]P. Jung, Phys. Rep. **234**, 175 (1993).
[9]I. Kh. Kaufman, G. G. Luchinsky, P. V. E. McClintock, S. M. Soskin, and N. D. Stein, Phys. Lett. A **220**, 219 (1996).
[10]Z. Gingl, L. B. Kiss, and F. Moss, Europhys. Lett. **29**, 191 (1995).
[11]J. M. G. Vilar, G. Gomila, and J. M. Rubi, Phys. Rev. Lett. **81**, 14 (1998).
[12]A. M. Glukhov, A. G. Sivakov, and A. V. Ustinov, Fiz. Nizk. Temp. **28**, 543 (2002) [Low Temp. Phys. **28**, 383 (2002)].
[13]R. Rouse, Siyuan Han, and J. E. Lukens, Appl. Phys. Lett. **66**, 108 (1995).
[14]A. D. Hibbs and A. L. Singsaas, J. Appl. Phys. **77**, 2582 (1995).
[15]A. D. Hibbs, R. E. Sager, D. W. Cox, T. H. Aukerman, T. A. Sage, and R. S. Landis, Rev. Sci. Instrum. **63**, 3652 (1992).
[16]R. V. Czipott and V. N. Podney, IEEE Trans. Magn. **25**(2), 1204 (1989).
[17]J. P. Wilkswo, Jr., IEEE Trans. Appl. Supercond. **5**, 74 (1995).
[18]V. I. Shnyrkov and Yu. P. Bliokh, in *XII Trilateral German–Russian–Ukrainian Seminar on High-Temperature Superconductivity*, Kiev, 25–29 October 1999, Program and Abstracts, p. 81.
[19]A. Neiman and L. Schimansky-Geier, Phys. Lett. A **197**, 379 (1995).
[20]V. A. Khlus, A. N. Omel'yanchuk, and I. O. Kulik, Fiz. Nizk. Temp. **5**, 118 (1979) [Sov. J. Low Temp. Phys. **5**, 55 (1979)]; K. K. Likharev, Rev. Mod. Phys. **51**, 101 (1979).
[21]A. Barone and G. Paterno, *Physics and Applications of the Josephson Effect*, Wiley, New York (1982), Mir, Moscow (1984).
[22]S. M. Frolov, D. J. Van Harlingen, V. A. Oboznov, V. V. Bolginov, and V. V. Ryazanov, Phys. Rev. B **70**, 144505 (2004).
[23]H. A. Kramers, Physica (Amsterdam) **7**, 284 (1940).
[24]R. de Bruyn Ouboter and A. N. Omelyanchouk, Superlattices Microstruct. **25**, 1005 (1999).
[25]O. G. Turutanov, A. N. Omelyanchouk, V. I. Shnyrkov, and Yu. P. Bliokh, Physica C **372–376**, 237 (2002).

Translated by Steve Torstveit